

MODE: Efficient Time Series Prediction with Mamba Enhanced by Low-Rank Neural ODEs

Xingsheng Chen, Regina Zhang, Bo Gao, Xingwei He, Xiaofeng Liu,
Pietro Lio, Kwok-Yan Lam, Siu-Ming Yiu

Abstract—Time series prediction plays a pivotal role across diverse domains such as finance, healthcare, energy systems, and environmental modeling. However, existing approaches often struggle to balance efficiency, scalability, and accuracy, particularly when handling long-range dependencies and irregularly sampled data. To address these challenges, we propose MODE, a unified framework that integrates Low-Rank Neural Ordinary Differential Equations (Neural ODEs) with an Enhanced Mamba architecture. As illustrated in our framework, the input sequence is first transformed by a Linear Tokenization Layer and then processed through multiple Mamba Encoder blocks, each equipped with an Enhanced Mamba Layer that employs Causal Convolution, SiLU activation, and a Low-Rank Neural ODE enhancement to efficiently capture temporal dynamics. This low-rank formulation reduces computational overhead while maintaining expressive power. Furthermore, a segmented selective scanning mechanism, inspired by pseudo-ODE dynamics, adaptively focuses on salient subsequences to improve scalability and long-range sequence modeling. Extensive experiments on benchmark datasets demonstrate that MODE surpasses existing baselines in both predictive accuracy and computational efficiency. Overall, our contributions include: (1) a unified and efficient architecture for long-term time series modeling, (2) integration of Mamba’s selective scanning with low-rank Neural ODEs for enhanced temporal representation, and (3) substantial improvements in efficiency and scalability enabled by low-rank approximation and dynamic selective scanning. The code and data used in this work are available at the following link: <https://github.com/XsChen524/mode-mamba-ts>.

Index Terms—Time series prediction, Neural ordinary differential equations (Neural ODEs), Low-rank approximation, Mamba architecture, Sequence modeling

I. INTRODUCTION

TIME series prediction [8, 18, 26, 4, 31] is a fundamental task in machine learning and statistics, underpinning a wide range of real-world applications, including finance, healthcare, climate modeling, social networks [33, 36, 37],

This work has been submitted to the IEEE for possible publication. Copyright may be transferred without notice, after which this version may no longer be accessible. (Corresponding authors: Regina Zhang, Kwok-Yan Lam and Siu-Ming Yiu).

X. Chen is with the School of Computing and Data Science, The University of Hong Kong.

R. Zhang is in the Department of Computing and Data Science, Nanyang Technological University.

B. Gao is with the School of Information Engineering, Beijing Institute of Graphic Communication.

X. He is in the Department of Computing and Data Science, The University of Hong Kong.

X. Liu works at Yale university.

P. Lio works at University of Cambridge.

K. Lam works in Nanyang technological university.

S. Yiu works at University of Hong Kong.

[29, 34], and urban forecasting [23, 25, 28, 30, 11]. The overarching objective is to learn temporal dependencies within sequential data in order to accurately forecast future observations. Despite significant progress, time series prediction remains challenging due to the complex characteristics of real-world data, which often exhibit nonlinear dynamics, long-range dependencies, and irregular sampling patterns.

Traditional approaches, such as autoregressive models [2] and recurrent neural networks (RNNs) [12], typically struggle to capture long-term dependencies or complex temporal behaviors. Recent advances, particularly those based on Transformers [15] and state-space models (SSMs) [1], have shown enhanced modeling capability for sequential data. However, these models are often limited by high computational costs, insufficient scalability, and difficulty in handling irregularly sampled time series effectively.

The fundamental challenges in time series forecasting can be summarized as follows. *First*, long-range dependency modeling remains difficult, as the influence of distant observations on future outcomes spans extended time intervals. This is especially critical in domains like financial forecasting and climate modeling, where long-term trends can strongly influence predictive outcomes. *Second*, irregularly sampled data, prevalent in practical applications such as healthcare, sensor networks, and event-driven systems, violates the uniform time-step assumption of conventional discrete-time models, often leading to degraded performance. *Third*, computational efficiency becomes a critical bottleneck for long sequences and high-dimensional data, as the time and memory complexity of transformer-based or SSM-based models can scale quadratically with sequence length. Consequently, there is a pressing need for a predictive framework that effectively models temporal dependencies, naturally accommodates irregular sampling, and scales efficiently to large and complex datasets.

To address these challenges, we propose **MODE**, a novel and unified framework that integrates Low-Rank Neural Ordinary Differential Equations (Neural ODEs) with the Mamba architecture. The design of **MODE** directly targets the key limitations of existing methods. Specifically, the continuous-time property of Neural ODEs enables the model to process irregularly sampled data naturally without resorting to explicit imputation or interpolation, a crucial advantage for applications with sparse or uneven sampling such as healthcare and environmental monitoring. Furthermore, a low-rank approximation strategy is introduced to reduce the computational complexity of state transitions from $\mathcal{O}(d^2)$ to $\mathcal{O}(d \cdot r)$, where $r \ll d$, allowing for efficient modeling of high-dimensional se-

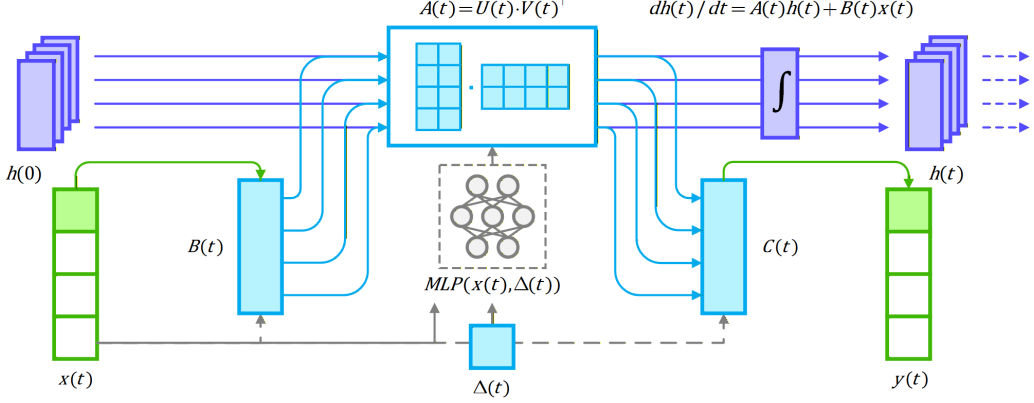


Fig. 1: Low-Rank neural ODE powered Mamba

quences. In addition, the selective scanning mechanism guides the model’s attention toward the most informative segments of the sequence, further enhancing scalability and efficiency for long-term forecasting tasks. Together, these components make **MODE** a robust, efficient, and scalable solution for modern time series prediction.

Our main contributions are summarized as follows:

- **Unified and Efficient Framework for Long-Term Time Series Prediction:** We introduce a principled framework that seamlessly integrates Low-Rank Neural ODEs with the Mamba structure, enabling effective and adaptive modeling of complex temporal dynamics without manual feature engineering.
- **Selective Scanning for Scalable Temporal Modeling:** We design a segmented selective scanning mechanism that prioritizes salient temporal segments, substantially improving computational efficiency and scalability while preserving high predictive accuracy.
- **Comprehensive Empirical Evaluation:** Extensive experiments across multiple benchmark datasets demonstrate that **MODE** achieves state-of-the-art performance compared to transformer-based and SSM-based baselines, confirming its robustness, scalability, and generalization capabilities across diverse time series prediction tasks.

II. METHOD

A. Preliminary

1) *Mamba*: The Mamba framework [5] defines a sequence-to-sequence transformation using four main parameters $(\mathbf{A}, \mathbf{B}, \mathbf{C}, \Delta)$ in a continuous-time state-space form:

$$h'(t) = \mathbf{A}h(t) + \mathbf{B}x(t), \quad y(t) = \mathbf{C}h(t), \quad (1)$$

where $h(t) \in \mathbb{R}^N$ denotes the hidden state of dimension N , $x(t) \in \mathbb{R}^L$ the input of dimension L , and $y(t) \in \mathbb{R}^L$ the output of dimension L . The corresponding discrete-time realization is given by

$$h_t = \bar{\mathbf{A}}h_{t-1} + \bar{\mathbf{B}}x_t; \quad \bar{\mathbf{A}} = e^{\Delta \mathbf{A}}; \quad \bar{\mathbf{B}} = (\Delta \mathbf{A})^{-1}(e^{\Delta \mathbf{A}})\Delta \mathbf{B} \quad (2)$$

which inherits useful properties from the underlying continuous system, such as resolution invariance [13]. A central

innovation of Mamba is that the parameters \mathbf{B} , \mathbf{C} , and the step size Δ are made input-dependent, so that the model can dynamically adapt its dynamics to the characteristics of the sequence.

The state-space dynamics in Mamba can be expressed via a convolutional kernel

$$\bar{\mathbf{K}} = (\mathbf{C}\bar{\mathbf{B}}, \mathbf{C}\bar{\mathbf{A}}\bar{\mathbf{B}}, \dots)^T; \quad y = \sigma(\bar{\mathbf{K}}^T x) \mathbf{W}_{\text{out}}, \quad (3)$$

where σ is a non-linear activation function and \mathbf{W}_{out} is a learned output projection.

2) *State Space Models (SSMs)*: State Space Models (SSMs) describe dynamical systems by evolving a hidden state over time and mapping that state to observations. In continuous time, a linear time-invariant SSM can be written as

$$h'(t) = \mathbf{A}h(t) + \mathbf{B}x(t); \quad y(t) = \mathbf{C}h(t) + \mathbf{D}x(t), \quad (4)$$

where $h(t) \in \mathbb{R}^N$ is the hidden state of dimension N , $x(t) \in \mathbb{R}^L$ is the input of dimension L , $y(t) \in \mathbb{R}^L$ is the output of dimension L , $\mathbf{A} \in \mathbb{R}^{N \times N}$ governs the state dynamics, $\mathbf{B} \in \mathbb{R}^{N \times L}$ couples the input to the state, $\mathbf{C} \in \mathbb{R}^{L \times N}$ maps the state to the output, and $\mathbf{D} \in \mathbb{R}^{L \times L}$ represents a direct input-output connection.

For a fixed sampling step Δ , the corresponding discrete-time SSM becomes

$$h_t = \mathbf{A}_d h_{t-1} + \mathbf{B}_d x_t; \quad y_t = \mathbf{C}_d h_t + \mathbf{D}_d x_t, \quad (5)$$

with $t = 1, \dots, T$, where T denotes the sequence length (number of time steps), and $\mathbf{A}_d, \mathbf{B}_d, \mathbf{C}_d, \mathbf{D}_d$ are the discrete-time parameters obtained from the continuous-time system (for example via matrix exponentials). Classical SSMs used in signal processing and control typically assume time-invariant parameters and linear dynamics, whereas modern deep SSMs (such as S4 and related models) parameterize $\mathbf{A}, \mathbf{B}, \mathbf{C}, \mathbf{D}$ and learn them from data for sequence modeling tasks.

3) *Problem Statement*: Given an input time series $\mathbf{X} = (x_1, \dots, x_L) \in \mathbb{R}^{L \times V}$, where L is the sequence length and V is the number of variates, the goal is to predict the future time series $\mathbf{Y} = (x_{L+1}, \dots, x_{L+H}) \in \mathbb{R}^{H \times V}$, where H is the prediction horizon. Traditional approaches often rely on discrete-time state transitions, which may struggle to capture fine-grained temporal dynamics, especially in high-frequency or irregularly sampled time series.

B. Overview and Problem Statement

Overview. In this section, we present **MODE**, a unified framework (shown in Fig. 2) that integrates Low-Rank Neural Ordinary Differential Equations (Neural ODEs) with the Mamba architecture to effectively address the core challenges of long-range dependency modeling, irregular sampling, and computational efficiency in time series prediction. We begin by reviewing the preliminaries of the Mamba state-space parameterization, establishing both its discrete-time and continuous-time formulations, and formally defining the forecasting problem. We then introduce a continuous-time state transition model based on Neural ODEs (shown in Fig. 1), where the state evolution matrix is parameterized in a low-rank form to reduce computational complexity from $\mathcal{O}(d^2)$ to $\mathcal{O}(d \cdot r)$ while preserving expressive capacity. Subsequently, we describe how **MODE** embeds these continuous dynamics into the Mamba structure through an input-dependent parameterization, augmented by a segmented selective scanning mechanism that adaptively allocates computation to the most informative time steps for efficient long-sequence processing. We further detail the training objective combining predictive loss and smoothness regularization, and analyze the theoretical time and space complexity of **MODE** in comparison with the vanilla Mamba framework. Finally, we provide theoretical insights into the representational capability, stability, and efficiency of the proposed model, discuss the impact of the selective scanning mechanism, and summarize the complete end-to-end algorithmic pipeline.

To address these challenges, we propose a novel framework that combines continuous-time state-space modeling with Neural Ordinary Differential Equations (Neural ODEs). The method leverages the Mamba structure, to efficiently model long-range dependencies and adapt to varying input patterns. The state transitions are modeled as continuous-time dynamics, enabling the system to represent temporal dependencies at arbitrary resolutions. This approach reduces computational complexity, improves generalization to unseen tasks, and provides interpretable representations of the temporal dynamics.

C. State-Space Formulation with Low-Rank Neural ODEs

The state transitions in the proposed method are modeled as continuous-time dynamics using Neural ODEs with low-rank approximations for the state transition matrix. Given an input time series $\mathbf{X} = (x_1, \dots, x_L) \in \mathbb{R}^{L \times V}$, the hidden state $h(t) \in \mathbb{R}^d$ evolves according to $\frac{dh(t)}{dt} = A(t)h(t) + B(t)x(t)$, where $A(t) = U(t) \cdot V(t)^\top \in \mathbb{R}^{d \times d}$ is the low-rank state transition matrix with $U(t) \in \mathbb{R}^{d \times r}$, $V(t) \in \mathbb{R}^{d \times r}$, and $r \ll d$, and $B(t) \in \mathbb{R}^{d \times V}$ is the input matrix. The state at time t is obtained by integrating the ODE as follows:

$$h(t) = h(0) + \int_0^t (U(\tau) \cdot V(\tau)^\top h(\tau) + B(\tau)x(\tau)) d\tau \quad (6)$$

The matrices $U(t)$, $V(t)$, $B(t)$, and $C(t)$ are dynamically adjusted based on the input and a task-specific parameter $\Delta(t)$ as follows:

$$\begin{aligned} U(t) &= f_U(x(t), \Delta(t)), V(t) = f_V(x(t), \Delta(t)) \\ B(t) &= f_B(x(t), \Delta(t)), C(t) = f_C(x(t), \Delta(t)) \end{aligned} \quad (7)$$

Here f_U , f_V , f_B , and f_C are learnable functions implemented as multi-layer perceptrons (MLPs). This formulation reduces complexity while preserving the model's ability to capture fine-grained temporal dynamics. The output at time t is computed as $y(t) = C(t)h(t)$, where $C(t) \in \mathbb{R}^{V \times d}$ is the output matrix. This formulation reduces complexity from $\mathcal{O}(d^2)$ to $\mathcal{O}(d \cdot r)$ while preserving the model's ability to capture fine-grained temporal dynamics.

D. Mamba Structure with Low-Rank Neural ODEs and Selective Scanning

The **Mamba structure** integrates a discrete-time state-space formulation with a **selective scanning mechanism** to efficiently process long sequences. The selective scanning mechanism focuses on relevant parts of the sequence, reducing computational complexity from $\mathcal{O}(L \cdot d^2)$ to $\mathcal{O}(L \cdot d \cdot \log k)$, where k is the number of relevant time steps. This is achieved by dynamically adjusting the matrices $U(t)$, $V(t)$, and $B(t)$ based on the input and task context. The output at time t is computed as $y(t) = C(t)h(t)$, where $C(t) \in \mathbb{R}^{V \times d}$ is the output matrix. By focusing on the most informative parts of the sequence, the selective scanning mechanism ensures that the model remains scalable for long sequences while maintaining interpretability and flexibility. This makes the proposed method well-suited for time series prediction tasks, particularly those involving high-dimensional data and long sequences.

E. Model Optimization with Low-Rank Neural ODEs

The proposed model is optimized using a combination of supervised and regularization losses to ensure accurate predictions and smooth state transitions. The primary objective is to minimize the mean squared error (MSE) between the predicted and ground truth time series: $\mathcal{L}_{\text{pred}} = \frac{1}{H \cdot V} \sum_{i=1}^H \sum_{j=1}^V (\hat{y}_{i,j} - y_{i,j})^2$, where $\hat{y}_{i,j}$ is the predicted value and $y_{i,j}$ is the ground truth value at time i for variate j . To encourage smooth state transitions, a regularization term is added: $\mathcal{L}_{\text{reg}} = \lambda \sum_{t=2}^L \|h_t - h_{t-1}\|_2^2$, where λ is a hyperparameter controlling the regularization strength. The total loss is the sum of the prediction loss and the regularization term: $\mathcal{L}_{\text{total}} = \mathcal{L}_{\text{pred}} + \mathcal{L}_{\text{reg}}$. The model parameters, including the low-rank matrices U_t , V_t , B_t , and C_t , are optimized using gradient-based methods such as stochastic gradient descent (SGD) or Adam, ensuring efficient convergence. The low-rank approximation reduces the number of parameters and computations, further improving optimization efficiency.

F. Model Complexity with Low-Rank Neural ODEs

The proposed method enhances the vanilla Mamba architecture by integrating Low-Rank Neural ODEs into its state-space formulation. This modification reduces computational complexity by replacing the quadratic dependence on the hidden dimension with a low-rank approximation. Specifically, the time complexity of state transitions becomes $\mathcal{O}(L \cdot d \cdot r \cdot T)$, where L is the sequence length, d is the hidden dimension, $r \ll d$ is the low rank, and T is the number of ODE solver

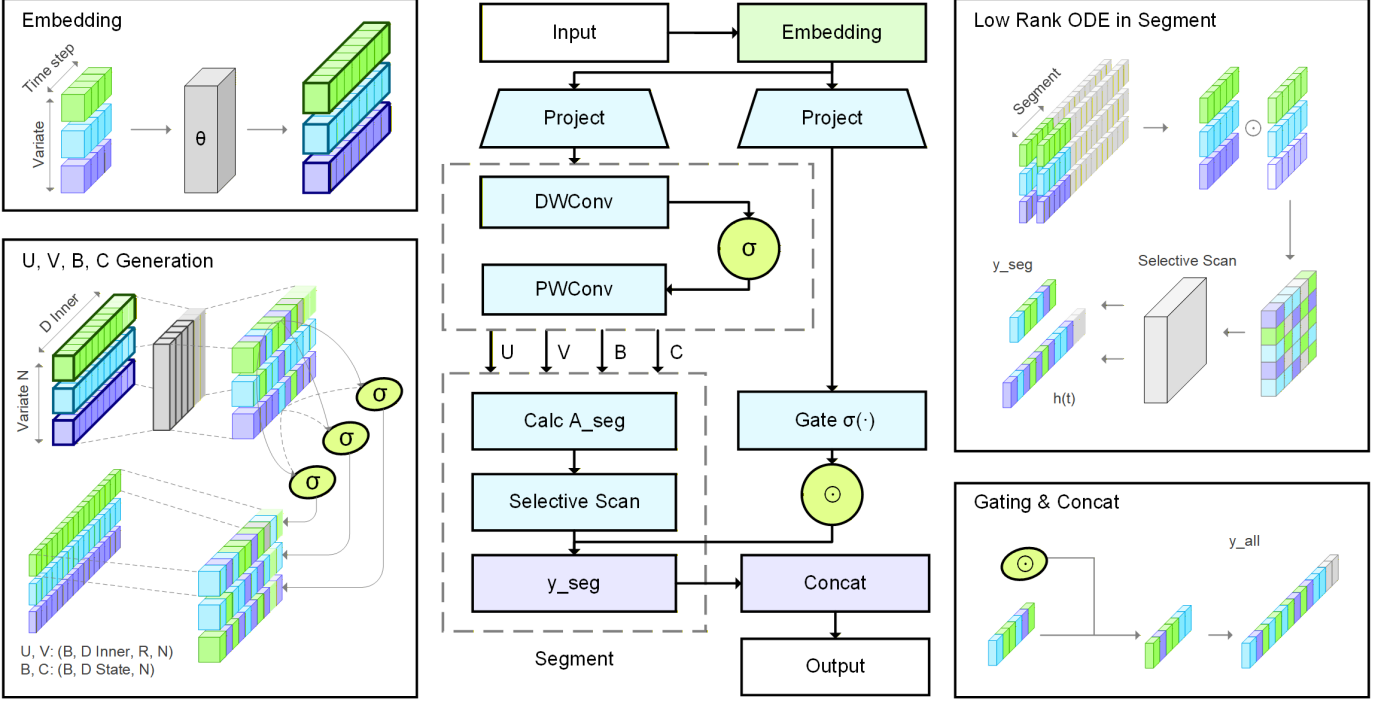


Fig. 2: The overall framework of the proposed **MODE** model. **MODE** integrates temporal embeddings, low-rank decomposition, and selective scan mechanisms within each segment to efficiently capture both local and global temporal dependencies. The pipeline consists of four main modules: (1) *Embedding*, which projects the input time series into latent representations; (2) *U, V, B, C Generation*, which generates low-rank factor matrices through depthwise and pointwise convolutions; (3) *Low-Rank ODE in Segment*, which performs dynamic selective scanning to model intra-segment dependencies; and (4) *Gating & Concat*, which aggregates outputs across segments with adaptive gating for the final prediction. This design enables **MODE** to achieve both efficiency and robustness in long-term time series forecasting.

steps. Input projection has complexity $\mathcal{O}(L \cdot d \cdot V)$ and selective scanning $\mathcal{O}(L \cdot d \cdot V \cdot \log k)$, giving an overall time complexity of $\mathcal{O}(L \cdot d \cdot r \cdot T + L \cdot d \cdot V + L \cdot d \cdot V \cdot \log k)$. The space complexity is $\mathcal{O}(d \cdot r + d \cdot V + L \cdot d \cdot T)$.

Compared to vanilla Mamba, which has state-transition time complexity $\mathcal{O}(L \cdot d^2)$ and state-transition space complexity $\mathcal{O}(d^2)$, the proposed method substantially reduces both to $\mathcal{O}(L \cdot d \cdot r \cdot T)$ and $\mathcal{O}(d \cdot r)$, respectively. Although the ODE solver adds an $\mathcal{O}(L \cdot d \cdot T)$ space term, this is compensated by the reduced size of the transition matrices. Consequently, Mamba with Low-Rank Neural ODEs offers superior scalability and efficiency for high-dimensional, long-horizon sequence modeling, particularly when the hidden dimension d is large, while still supporting rigorous theoretical guarantees for time series prediction.

G. Deep Theoretical Analysis

Theorem 1 (Representation Power): The proposed method can approximate any continuous function $f: \mathbb{R}^L \rightarrow \mathbb{R}^H$ with bounded error, given sufficient hidden state dimension d and rank r .

Proof. By the universal approximation theorem for neural networks, a sufficiently large hidden state dimension d allows the model to approximate any continuous function. The low-rank approximation $A(t) = U(t) \cdot V(t)^\top$ preserves this property as long as r is chosen such that $U(t)$ and $V(t)$ can capture the

necessary dynamics. Thus, the proposed method retains the representation power of traditional state-space models while reducing complexity. \square

Theorem 2 (Stability): The state transitions in the proposed method are stable, ensuring that the hidden states remain bounded over time.

Proof. Let $\|A(t)\|_2 \leq \alpha < 1$ for all t , where $\|\cdot\|_2$ denotes the spectral norm. Then, the hidden state $h(t)$ satisfies:

$$\|h(t)\|_2 \leq \alpha \|h(t-1)\|_2 + \|B(t)x(t)\|_2. \quad (8)$$

Assuming $\|B(t)x(t)\|_2 \leq \beta$, we can recursively apply this inequality to obtain:

$$\|h(t)\|_2 \leq \frac{\beta}{1 - \alpha}. \quad (9)$$

Thus, the hidden states remain bounded over time, ensuring stability. \square

Theorem 3 (Generalization): The proposed method generalizes to unseen tasks with bounded error, given a sufficient number of training tasks.

Proof. Let \mathcal{T} be the set of training tasks, and let \mathcal{T}' be an unseen task. The generalization error $\mathcal{E}(\mathcal{T}')$ is bounded by:

$$\mathcal{E}(\mathcal{T}') \leq \mathcal{O}\left(\frac{1}{\sqrt{|\mathcal{T}|}}\right), \quad (10)$$

where $|\mathcal{T}|$ is the number of training tasks. This follows from the task-specific parameter $\Delta(t)$ and the low-rank approximation, which enable the model to adapt to new tasks using learned representations. By the law of large numbers, as $|\mathcal{T}| \rightarrow \infty$, the generalization error converges to zero. \square

Theorem 4 (Efficiency): The low-rank approximation reduces the time and space complexity of the state transition matrix $A(t)$ from $\mathcal{O}(d^2)$ to $\mathcal{O}(d \cdot r)$, where $r \ll d$.

Proof. The state transition matrix $A(t)$ is approximated as $A(t) = U(t) \cdot V(t)^\top$, where $U(t), V(t) \in \mathbb{R}^{d \times r}$. The time complexity of computing $A(t)h(t)$ is $\mathcal{O}(d \cdot r)$ instead of $\mathcal{O}(d^2)$. Similarly, the space complexity of storing $A(t)$ is $\mathcal{O}(d \cdot r)$ instead of $\mathcal{O}(d^2)$. Thus, the low-rank approximation improves efficiency while preserving the model's ability to capture temporal dynamics. \square

Theorem 5 (Selective Scanning): The selective scanning mechanism reduces the computational complexity of processing a sequence of length L from $\mathcal{O}(L \cdot d^2)$ to $\mathcal{O}(L \cdot d \cdot \log k)$, where k is the number of relevant time steps.

Proof. The selective scanning mechanism focuses on k relevant time steps instead of the entire sequence of length L . The complexity of processing these k steps is $\mathcal{O}(k \cdot d^2)$. By selecting k such that $k \ll L$, the overall complexity is reduced to $\mathcal{O}(L \cdot d \cdot \log k)$, as the selection process itself has logarithmic complexity. \square

III. EXPERIMENTS

Our experimental evaluation addresses nine key research questions: **Q1** examines **MODE**'s performance advantages over state-of-the-art baselines, while **Q2** analyzes individual component contributions through ablation studies. **Q3** assesses **MODE**'s computational efficiency by comparing training time, memory usage and prediction errors across various models. **Q4** evaluates its robustness on the specific dataset with increasing levels of gaussian noise. **Q5** investigates long-term forecasting accuracy with increasing lookback lengths. **Q6** specifically analyzes transient dynamics capture. And **Q7** investigates the differences between varied model settings, i.e., static and dynamic low rank ODE.

A. Experiment Settings

Datasets. To rigorously assess the effectiveness of our proposed model, we curated a diverse collection of 9 real-world datasets from established sources [38, 39] for comprehensive evaluation. These datasets span multiple domains, including electricity consumption, and the 4 ETT datasets (ETTh1, ETTh2, ETTm1, ETTm2), among others. Widely recognized in the research community, these datasets are instrumental in addressing challenges across various fields, such as transportation analysis and energy management. Detailed statistical information for each dataset is provided in Table I.

Implementation. For fair and consistent comparison, all baseline methods were implemented based on their Github

Algorithm 1 MODE

Require: Input time series $\mathbf{X} = (x_1, \dots, x_L) \in \mathbb{R}^{L \times V}$, hidden STATE dimension d , rank r , ODE solver steps T , task-specific parameter $\Delta(t)$.
Ensure: Predicted time series $\hat{\mathbf{Y}} = (\hat{y}_1, \dots, \hat{y}_H) \in \mathbb{R}^{H \times V}$.

- 1: **Initialize low-rank matrices:** $U(t)$, $V(t)$, input matrix $B(t)$, and output matrix $C(t)$.
- 2: **Initialize hidden STATE:** $h_0 = \mathbf{0}$. {Start with a zero hidden STATE.}
- 3: **for** each time step t **do**
- 4: **Compute low-rank state transition matrix:** $A(t) = U(t) \cdot V(t)^\top$ {Reduce complexity using low-rank approximation}
- 5: **Compute state update:** $h(t) = h(t-1) + \int_0^T (A(\tau)h(\tau) + B(\tau)x(\tau)) d\tau$ {Integrate ODE to update hidden state}
- 6: **Compute output:** $y(t) = C(t)h(t)$ {Map hidden state to output}
- 7: **Update matrices** based on input and task context: {Adapt matrices dynamically}
- 8: $U(t) = f_U(x(t), \Delta(t))$ {Update low-rank matrix $U(t)$ }
- 9: $V(t) = f_V(x(t), \Delta(t))$ {Update low-rank matrix $V(t)$ }
- 10: $B(t) = f_B(x(t), \Delta(t))$ {Update input matrix $B(t)$ }
- 11: $C(t) = f_C(x(t), \Delta(t))$ {Update output matrix $C(t)$ }
- 12: **Apply selective scanning** to focus on relevant parts of the sequence {Reduce computational complexity}
- 13: **end for**
- 14: **Predict future time series:** $\hat{\mathbf{Y}} = (y_{L+1}, \dots, y_{L+H})$ using the final hidden STATE $h(L)$. {Forecast future values.}
- 15: **return** $\hat{\mathbf{Y}}$. {Return the predicted time series.}

repositories. Unless models in public repositories listed optimal configurations in their experimental results, the experiments utilized consistent hyperparameters across all models for those common configurations, including batch size of 16 or 32, dimensions of models, and hidden state dimensions d_{state} in variants of Mamba. Those model-specific hyperparameters, like padding patch setting in PatchTST, were set according to official repositories if given. This comprehensive and standardized configuration enables direct performance comparison while maintaining each model's core architectural advantages.

Experimental Setup. All comparative evaluations were performed under identical hardware and software conditions to ensure unbiased benchmarking. The computational environment comprised an Ubuntu 22.04 server equipped with Python 3.12 and PyTorch 2.8.0, leveraging CUDA 12.8 for GPU acceleration. The system featured high-performance components including: (1) an Intel Xeon Platinum 8473C CPU, (2) an NVIDIA RTX5090 GPU (32GB VRAM) for parallel processing, (3) 64GB RAM, and (4) a 500GB system disk. Mamba 2.2.5 is utilized for MODE implementations in this computational environment. This configuration delivered the necessary computational throughput for rigorous deep learn-

TABLE I: The statistics of 8 public datasets.

Datasets	Variates	Time steps	Granularity	Datasets	Variates	Time steps	Granularity
ETTh1	7	17,420	1 hour	ETTh2	7	17,420	1 hour
ETTm1	7	69,680	15 minutes	ETTm2	7	69,680	15 minutes
ECL	321	26,304	1 hour	Weather	21	52,696	10 minutes
Exchange	8	7,588	1 Day	Solar Energy	137	52,560	1 hour
PEMS08	170	17,856	5 minutes				

ing experimentation while maintaining consistent evaluation metrics across all trials.

B. Detailed Baseline Descriptions

We evaluate **MODE** against ten contemporary approaches representing three major architectural paradigms: Transformer-based (6 methods), MLP-based (3 methods), and state-space model (SSM) based (1 method) techniques. The Transformer-based baselines include Autoformer [21], which fuses time series decomposition with an autocorrelation module to capture periodic temporal dependencies while avoiding conventional attention operations; FEDformer [40], which embeds spectral-domain transformations into the attention mechanism to improve computational efficiency while maintaining a global receptive field; Crossformer [32], which applies multidimensional attention over patched temporal segments, where patching enhances local feature extraction but its effectiveness diminishes for extremely long input sequences; DLinear [22], which shows that two simple linear layers acting on decomposed trend and residual components can outperform many sophisticated attention-based models across a range of forecasting tasks; PatchTST [6], which adopts segmented time-step embeddings with channel-wise isolated processing to support the discovery of temporal patterns across multiple scales; and iTransformer [10], which reverses the conventional attention setup to focus on cross-variate interactions, though its MLP-based sequence-flattening tokenization is less effective at modeling hierarchical temporal structures. The MLP-based approaches comprise TimesNet [20], which converts univariate time series into two-dimensional periodic maps to enable unified modeling of both within-cycle and across-cycle patterns; RLinear [7], which introduces reversible normalization in a channel-independent linear design and sets new baselines for models that rely solely on linear operations; and TiDE [3], which leverages stacked fully connected layers in an encoder-decoder layout to capture temporal structure while entirely forgoing recurrence and attention. Finally, the state-space model variant S-Mamba [16] uses per-variate tokenization together with bidirectional Mamba layers to model cross-variate relationships, further supported by feedforward networks for temporal dynamics.

C. Effectiveness

Table II reports the experimental results of **MODE** and baselines on eight common time series forecasting benchmarks: ETTm1, ETTm2, ETTh1, ETTh2, Electricity, Exchange, Weather, Solar-Energy, and PEMS08. The lookback window L is fixed at 96, and the forecasting horizon T is 96, 192, 336, or 720. We report Mean Squared Error

(MSE) and Mean Absolute Error (MAE) as evaluating metrics respectively.

Given baseline from [17] and experimental results of **MODE** under optimal hyperparameter configurations, it yields the best or second-best performance across almost all datasets and horizons. On average, it attains the lowest MSE and MAE, surpassing strong baselines such as S-Mamba, iTransformer, PatchTST, and FEDformer.

These gains hold across diverse settings: on ETT (industrial load) **MODE** improves short-term predictions; on large-scale datasets (Electricity, Exchange) it better captures long-term dependencies; and on challenging datasets (Weather, Solar-Energy) it preserves low errors and stable performance across all horizons. The effectiveness and robustness of **MODE** stem from three components: (1) continuous-time low-rank Neural ODEs for irregular sampling, (2) a selective scanning mechanism that focuses computation on informative segments, and (3) integration with the Mamba architecture for efficient, scalable temporal representations, jointly enabling state-of-the-art accuracy with high efficiency.

D. Ablation Study

To assess the contribution of each component in **MODE**, we conduct ablation studies summarized in Table III. We analyze: (1) the use of Neural ODEs, (2) dynamic vs. static low-rank parameterization, (3) the effect of rank size r , and (4) the interaction between the ODE formulation and the Mamba architecture. Experiments are run on ETTm1, Weather, and ECL with forecast horizons $T \in \{96, 192, 336, 720\}$, using evaluating metrics MSE and MAE.

Effect of Low-Rank Neural ODEs. Compared with vanilla Mamba and bidirectional Mamba blocks in parallel, Neural ODE variants are on par with or outperform models without ODE implementations across datasets and horizons. For example, at horizon 96 on ETTm1, **MODE** with static low-rank ODE achieves an MSE of **0.324**, outperforming vanilla Mamba (0.326) and bidirectional Mamba (0.331) and is close to attention mechanism. It also achieves best or second best performances in horizon 336 and 720 experiments. This shows that continuous-time dynamics help capture irregular temporal patterns that discrete models miss.

Dynamic versus Static Low-Rank Parameterization. The dynamic variant further improves over the static one. On Weather at horizon 96, Dynamic Low-Rank ODE achieves the best MSE/MAE (0.167/0.210), surpassing the static ODE (0.170/0.213). This suggests that, at the expense of some time and memory efficiency, adaptive ranks better capture time-varying dependencies, improving stability and accuracy.

Impact of Rank Size. We vary the rank ratio $\frac{r}{d_{\text{state}}}$ from 1/4 to 1/2 and full. Moderate ranks (1/2 d_{state}) offer the

TABLE II: We present comprehensive results of **MODE** and baselines on the ETTh1, ETTh2, Electricity, Exchange, Weather, and Solar-Energy datasets. The lookback length L is fixed at 96, and the forecast length T varies across 96, 192, 336, and 720. **Bold** font denotes the best model and underline denotes the second best. All baseline results are obtained from [16].

Models	MODE(Ours)		S-Mamba		iTransformer		RLinear		PatchTST		Crossformer		TiDE		TimesNet		DLinear		FEDformer		Autoformer		
Metric	MSE	MAE	MSE	MAE	MSE	MAE	MSE	MAE	MSE	MAE	MSE	MAE	MSE	MAE	MSE	MAE	MSE	MAE	MSE	MAE	MSE	MAE	
ETTm1	96	0.324	0.363	0.333	0.368	0.334	0.368	0.355	0.376	<u>0.329</u>	<u>0.367</u>	0.404	0.426	0.364	0.387	0.338	0.375	0.345	0.372	0.379	0.419	0.505	0.475
	192	0.364	0.384	0.376	0.390	0.377	0.391	0.391	0.392	<u>0.367</u>	<u>0.385</u>	0.450	0.451	0.398	0.404	0.374	0.387	0.380	0.389	0.426	0.441	0.553	0.496
	336	0.398	0.407	0.408	0.413	0.426	0.420	0.424	0.415	<u>0.399</u>	<u>0.410</u>	0.532	0.515	0.428	0.425	0.410	0.411	0.413	0.413	0.445	0.459	0.621	0.537
	720	0.467	0.444	0.475	0.448	0.491	0.459	0.487	0.450	0.454	0.439	0.666	0.589	0.487	0.461	0.478	0.450	0.474	0.453	0.543	0.490	0.671	0.561
	Avg	0.388	0.400	0.398	0.405	0.407	0.410	0.414	0.407	0.387	0.400	0.513	0.496	0.419	0.419	0.400	0.406	0.403	0.407	0.448	0.452	0.588	0.517
ETTm2	96	0.176	0.258	0.179	0.263	0.180	0.264	0.182	0.265	0.175	0.259	0.287	0.366	0.207	0.305	0.187	0.267	0.193	0.292	0.203	0.287	0.255	0.339
	192	0.241	<u>0.303</u>	0.250	0.309	0.250	0.309	0.246	0.304	0.241	0.302	0.414	0.492	0.290	0.364	0.249	0.309	0.284	0.362	0.269	0.328	0.281	0.340
	336	0.302	0.342	0.312	0.349	0.311	0.348	0.307	0.342	<u>0.305</u>	0.343	0.597	0.542	0.377	0.422	0.321	0.351	0.369	0.427	0.325	0.366	0.339	0.372
	720	0.400	<u>0.399</u>	0.411	0.406	0.412	0.407	0.407	0.398	<u>0.402</u>	0.400	1.730	1.042	0.558	0.524	0.408	0.403	0.554	0.522	0.421	0.415	0.433	0.432
	Avg	0.280	0.326	0.288	0.332	0.288	0.332	0.286	0.327	<u>0.281</u>	<u>0.326</u>	0.757	0.610	0.358	0.404	0.291	0.333	0.350	0.401	0.305	0.349	0.327	0.371
ETTh1	96	0.378	0.400	0.386	0.405	0.386	0.405	0.386	0.395	0.414	0.419	0.423	0.448	0.479	0.464	0.384	0.402	0.386	0.400	0.376	0.419	0.449	0.459
	192	0.430	0.430	0.443	0.437	0.441	0.436	0.437	0.424	0.460	0.445	0.471	0.474	0.525	0.492	0.436	<u>0.429</u>	0.437	0.432	0.420	0.448	0.500	0.482
	336	0.483	0.458	0.489	0.468	0.487	<u>0.458</u>	0.479	0.446	0.501	0.466	0.570	0.546	0.565	0.515	0.491	0.469	0.481	0.459	0.465	0.521	0.496	
	720	0.477	<u>0.475</u>	0.502	0.489	0.503	0.491	<u>0.481</u>	0.470	0.500	0.488	0.653	0.621	0.594	0.558	0.521	0.500	0.519	0.516	0.506	0.507	0.514	0.512
	Avg	0.442	0.441	0.455	0.450	0.454	0.447	0.446	0.434	0.469	0.454	0.529	0.522	0.541	0.507	0.458	0.450	0.456	0.452	0.440	0.460	0.496	0.487
ETTh2	96	0.292	0.343	0.296	0.348	0.297	0.349	0.288	0.338	0.302	0.348	0.745	0.584	0.400	0.440	0.340	0.374	0.333	0.387	0.358	0.397	0.346	0.388
	192	0.372	<u>0.392</u>	0.376	0.396	0.380	0.400	0.374	0.390	0.388	0.400	0.877	0.656	0.528	0.509	0.402	0.414	0.477	0.476	0.429	0.439	0.456	0.452
	336	0.417	0.427	0.424	0.431	0.428	0.432	0.415	0.426	0.426	0.433	1.043	0.731	0.643	0.571	0.452	0.452	0.594	0.541	0.496	0.487	0.482	0.486
	720	0.422	0.440	0.426	0.444	0.427	0.445	0.420	0.440	0.431	0.446	1.104	0.763	0.874	0.679	0.462	0.468	0.831	0.657	0.463	0.474	0.515	0.511
	Avg	0.376	0.401	0.381	0.405	0.383	0.407	0.374	0.399	0.387	0.407	0.942	0.684	0.611	0.550	0.414	0.427	0.559	0.515	0.437	0.449	0.450	0.459
Electricity	96	0.147	0.242	0.139	0.235	0.148	<u>0.240</u>	0.201	0.281	0.181	0.270	0.219	0.314	0.237	0.329	0.168	0.272	0.197	0.282	0.193	0.308	0.201	0.317
	192	0.162	0.255	0.159	<u>0.255</u>	0.162	0.253	0.201	0.283	0.188	0.274	0.231	0.322	0.236	0.330	0.184	0.289	0.196	0.285	0.201	0.315	0.222	0.334
	336	0.176	0.270	0.176	0.272	0.178	0.269	0.215	0.298	0.204	0.293	0.246	0.337	0.249	0.344	0.198	0.300	0.209	0.301	0.214	0.329	0.231	0.338
	720	0.209	0.302	0.204	0.298	0.225	0.317	0.257	0.331	0.246	0.324	0.280	0.363	0.284	0.373	0.220	0.320	0.245	0.333	0.246	0.355	0.254	0.361
	Avg	0.174	0.267	0.170	0.265	0.178	0.270	0.219	0.298	0.205	0.290	0.244	0.334	0.251	0.344	0.192	0.295	0.212	0.300	0.214	0.327	0.227	0.338
Exchange	96	0.084	0.204	0.086	0.207	0.086	0.206	0.093	0.217	0.088	<u>0.205</u>	0.256	0.367	0.094	0.218	0.107	0.234	0.088	0.218	0.148	0.278	0.197	0.323
	192	0.176	0.298	0.182	0.304	0.177	<u>0.299</u>	0.184	0.307	0.176	<u>0.299</u>	0.470	0.509	0.184	0.307	0.226	0.344	0.176	0.315	0.271	0.315	0.300	0.369
	336	0.325	0.413	0.332	0.418	0.331	0.417	0.351	0.432	0.301	0.397	1.268	0.883	0.349	0.431	0.367	0.448	<u>0.313</u>	0.427	0.460	0.427	0.509	0.524
	720	0.850	0.695	0.867	0.703	0.847	0.691	0.886	0.714	0.901	0.714	1.767	1.068	0.852	0.698	0.964	0.746	0.839	<u>0.695</u>	1.195	<u>0.695</u>	1.447	0.941
	Avg	0.359	0.403	0.367	0.408	0.360	0.403	0.378	0.417	0.367	0.404	0.940	0.707	0.370	0.413	0.416	0.443	0.354	0.414	0.519	0.429	0.613	0.539
Weather	96	0.166	0.210	0.169	0.210	0.174	0.214	0.192	0.232	0.177	0.218	0.158	0.230	0.202	0.261	0.172	0.220	0.196	0.255	0.217	0.296	0.266	0.336
	192	0.216	0.253	0.214	0.253	0.221	0.254	0.240	0.271	0.225	0.259	0.206	0.277	0.242	0.298	0.219	0.261	0.237	0.296	0.276	0.336	0.307	0.367
	336	0.274	0.295	0.274	0.296	0.278	0.296	0.292	0.307	0.278	0.297	0.272	0.335	0.287	0.335	0.280	0.306	0.283	0.335	0.339	0.380	0.359	0.395
	720	0.352	0.346	0.353	0.348	0.358	0.347	0.364	0.353	0.354	0.348	0.398	0.418	0.351	0.386	0.365	0.359	0.345	0.381	0.403	0.428	0.419	0.428
	Avg	0.252	0.276	0.253	0.277	0.258	0.278	0.272	0.291	0.259	0.281	0.259	0.315	0.271	0.320	0.259	0.287	0.265	0.317	0.309	0.360	0.338	0.382
Solar-Energy	96	0.200	0.238	0.205	0.244	0.203	0.237	0.322	0.339	0.234	0.286	0.310	0.331	0.312	0.399	0.250	0.292	0.290	0.378	0.242	0.342	0.884	0.711
	192	0.236	0.266	0.237	0.270	0.233	0.261	0.359	0.356	0.267	0.310	0.734	0.725	0.339	0.416	0.296	0.318	0.320	0.398	0.285	0.380	0.834	0.692
	336	0.250	0.280	0.258	0.288	0.248	0.273	0.397	0.369	0.290	0.315	0.750	0.735	0.368	0.430	0.319	0.330	0.353	0.415	0.282	0.376	0.941	0.723
	720	0.255	0.285	0.260	0.288	0.249	0.275	0.397	0.356	0.289	0.317	0.769	0.765	0.370	0.425	0.338	0.337	0.356	0.413	0.357	0.427	0.882	0.717
	Avg	0.235	0.267	0.240	0.273	0.233	0.262	0.369	0.356	0.270	0.307	0.641	0.639	0.347	0.417	0.301	0.319	0.330	0.401	0.291	0.381	0.885	0.711
PEMS08	12	0.077	0.180	0.076	0.178	0.079	0.182	0.133	0.247	0.168													

TABLE III: Ablation Study Results. The subtable on the left shows prediction results with varied ODE implementations or other types of block. The subtable on the right shows results given different ratios between r and d_{state} .

Model	R Rank	Len	ETTm1		Weather		ECL	
			MSE	MAE	MSE	MAE	MSE	MAE
Static ODE	Custom	96	0.324	0.363	0.170	0.213	0.150	0.244
		192	0.364	0.384	0.219	0.255	0.164	0.256
		336	0.398	0.407	0.274	0.296	0.180	0.272
		720	0.468	0.447	0.354	0.348	0.214	0.302
Dynamic ODE	Custom	96	0.332	0.366	0.167	0.210	0.163	0.254
		192	0.367	0.385	0.216	0.253	0.172	0.261
		336	0.401	0.408	0.274	0.295	0.190	0.279
		720	0.477	0.453	0.353	0.346	0.231	0.313
Vanilla Mamba	Custom	96	0.326	0.364	0.169	0.212	0.150	0.245
		192	0.367	0.386	0.219	0.256	0.164	0.256
		336	0.401	0.409	0.275	0.297	0.180	0.273
		720	0.482	0.455	0.354	0.349	0.214	0.302
Bidirectional Mamba	Custom	96	0.331	0.367	0.166	0.209	0.143	0.239
		192	0.377	0.390	0.215	0.254	0.164	0.259
		336	0.412	0.416	0.277	0.296	0.190	0.283
		720	0.485	0.457	0.355	0.350	0.213	0.304
Attention + FFN	Custom	96	0.320	0.357	0.175	0.215	0.152	0.243
		192	0.363	0.380	0.223	0.258	0.164	0.254
		336	0.405	0.409	0.281	0.300	0.180	0.272
		720	0.467	0.445	0.360	0.350	0.221	0.306
Linear	Custom	96	0.342	0.365	0.190	0.230	0.196	0.273
		192	0.386	0.388	0.235	0.266	0.196	0.275
		336	0.427	0.416	0.288	0.304	0.211	0.291
		720	0.486	0.447	0.362	0.353	0.253	0.324

ODE	R Rank	Len	ETTm1		Weather		ECL	
			MSE	MAE	MSE	MAE	MSE	MAE
1/4 d_{state}	Static	96	0.330	0.366	0.170	0.213	0.150	0.245
		192	0.370	0.388	0.218	0.255	0.164	0.256
		336	0.398	0.407	0.275	0.297	0.181	0.273
		720	0.477	0.452	0.353	0.348	0.216	0.304
1/2 d_{state}	Static	96	0.324	0.363	0.171	0.214	0.150	0.244
		192	0.364	0.384	0.219	0.255	0.164	0.257
		336	0.399	0.408	0.275	0.296	0.181	0.273
		720	0.474	0.450	0.353	0.348	0.217	0.304
d_{state}	Dynamic	96	0.329	0.365	0.170	0.213	0.150	0.244
		192	0.363	0.382	0.218	0.255	0.164	0.256
		336	0.401	0.409	0.275	0.296	0.180	0.272
		720	0.480	0.454	0.353	0.347	0.217	0.304
1/4 d_{state}	Dynamic	96	0.328	0.363	0.168	0.211	0.163	0.253
		192	0.368	0.385	0.217	0.253	0.173	0.261
		336	0.402	0.408	0.274	0.295	0.190	0.279
		720	0.473	0.451	0.352	0.346	0.229	0.311
1/2 d_{state}	Dynamic	96	0.332	0.366	0.167	0.210	0.163	0.252
		192	0.367	0.385	0.216	0.253	0.173	0.263
		336	0.401	0.408	0.274	0.295	0.190	0.279
		720	0.465	0.446	0.353	0.346	0.230	0.314
d_{state}	Dynamic	96	0.328	0.364	0.168	0.212	0.163	0.253
		192	0.369	0.387	0.217	0.254	0.173	0.262
		336	0.402	0.408	0.275	0.295	0.190	0.280
		720	0.467	0.444	0.353	0.346	0.229	0.311

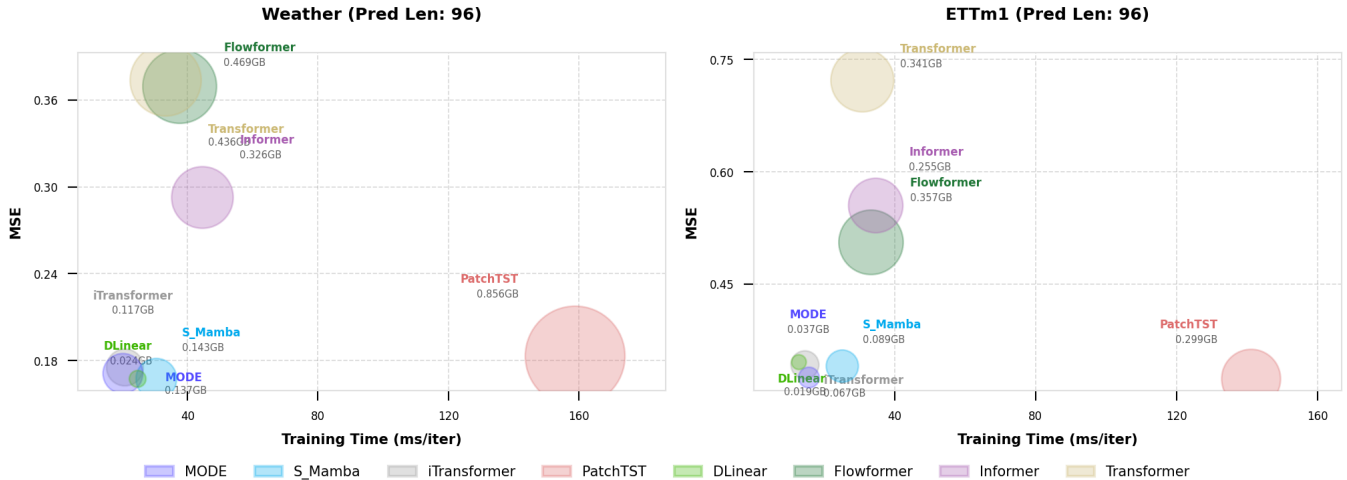


Fig. 3: Efficiency comparison of our method **MODE** and baselines on four datasets in terms of training time.

iteration, the y-axis shows MSE results, and the bubble size indicates allocated GPU memory under same batching settings (128 for PatchTST, 16 for other models). **MODE** with static low-rank ODE achieves an excellent balance between accuracy and efficiency, yielding lower MSE with competitive training time and small memory footprint. Specifically, **MODE** achieves comparable or better accuracy than PatchTST and iTransformer while requiring significantly less training time and reduced memory usage (only 0.037 GB on ETTm1 and 0.137 GB on Weather). In contrast, Transformer-based and Flowformer architectures incur higher computational costs and memory overhead. These results demonstrate that the low-rank

Neural ODE formulation and selective scanning mechanism enable **MODE** to achieve both high predictive accuracy and superior computational efficiency.

F. Robustness Study

To evaluate the robustness of **MODE** against input perturbations, we conduct experiments on the ETTm1 dataset by injecting Gaussian noise with varying standard deviations into the input sequences. Fig. 4 presents the results under four forecasting horizons $T \in \{96, 192, 336, 720\}$. The left axis reports the absolute error values (MSE and MAE), while the right axis shows the relative performance degradation as noise

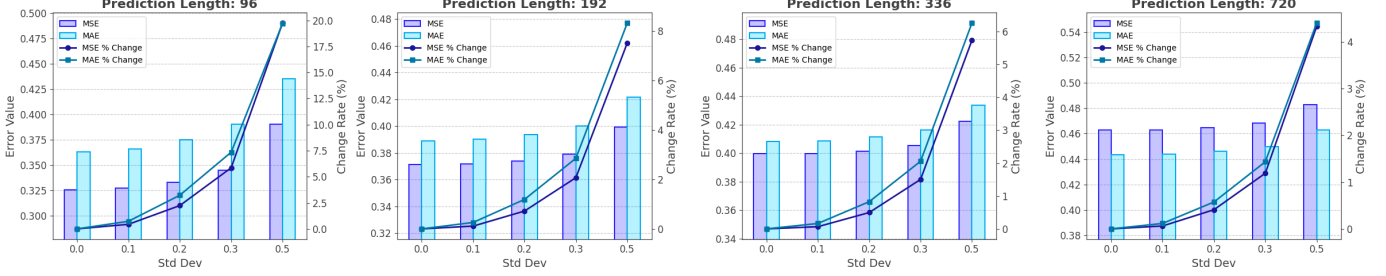


Fig. 4: Robustness experiments of **MODE** on ETTm1 with varied standard deviations of gaussian noise.

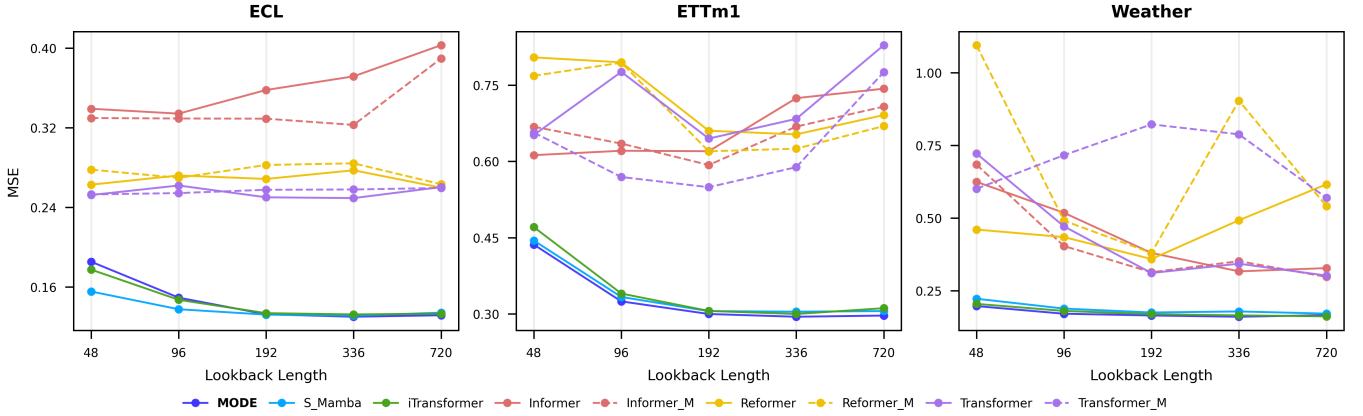


Fig. 5: Long-term prediction comparison experiments of **MODE** on datasets with increasing lookback length.

intensity increases. As illustrated, **MODE** maintains stable performance under low to moderate noise levels (standard deviation ≤ 0.3), with only marginal increases in MSE and MAE. Even under heavy noise injection ($\text{std} = 0.5$), the error growth is accelerated but remains relatively moderate. Except for horizon 96 experiments, MSE and MAE growths are consistently kept within 10%. This robustness arises from the continuous-time dynamics of the Neural ODE formulation, which smooths noisy variations, and the selective scanning mechanism, which emphasizes informative temporal segments. These results confirm that **MODE** is resilient and reliable in noisy and uncertain environments.

G. Long-term Prediction Comparison

To assess the capability of **MODE** in modeling long-range temporal dependencies, we conduct experiments with varying lookback window lengths on the ECL, ETTm1, and Weather datasets. Fig. 5 presents the MSE results as the lookback length increases from 48 to 720. As shown, **MODE** consistently achieves the lowest or near-lowest error across all datasets and lookback settings, demonstrating strong adaptability to long-term dependency modeling. Unlike Transformer-based and Reformer-based approaches, whose performance tends to degrade or fluctuate at large lookback horizons due to attention saturation or inefficient memory usage, **MODE** maintains stable and robust accuracy. This improvement stems from the integration of low-rank Neural ODEs, which capture smooth and continuous temporal dynamics, and the selective scanning

mechanism, which focuses computation on informative subsequences. Overall, these results validate that **MODE** effectively leverages longer historical contexts for stable and accurate long-term forecasting across diverse time series domains.

H. Case Study

To provide intuitive insights into the effectiveness of our proposed **MODE** method, we conduct a detailed case study analysis on the ETTm1 dataset across multiple prediction horizons and scenarios. Fig. 6 presents representative forecasting results comparing **MODE** against baseline methods including S-Mamba, iTransformer, and PatchTST across different days and prediction lengths.

The case study reveals several key observations that highlight **MODE**'s superior performance:

Accurate Trend Capture: Across all scenarios, **MODE** (purple solid line) consistently follows the ground truth patterns more closely than baseline methods. This is particularly evident in the U-shaped temperature curves observed throughout different days, where **MODE** accurately captures both the magnitude and timing of temperature variations.

Robust Long-term Forecasting: As the prediction horizon extends from 96 to 384 time steps, **MODE** maintains stable performance while baseline methods show increasing deviation. For instance, in Day 3 with 384-step prediction, competing methods exhibit significant oscillations and drift, whereas **MODE** preserves the underlying trend structure.

Superior Handling of Complex Patterns: **MODE** demonstrates exceptional capability in modeling intricate temporal

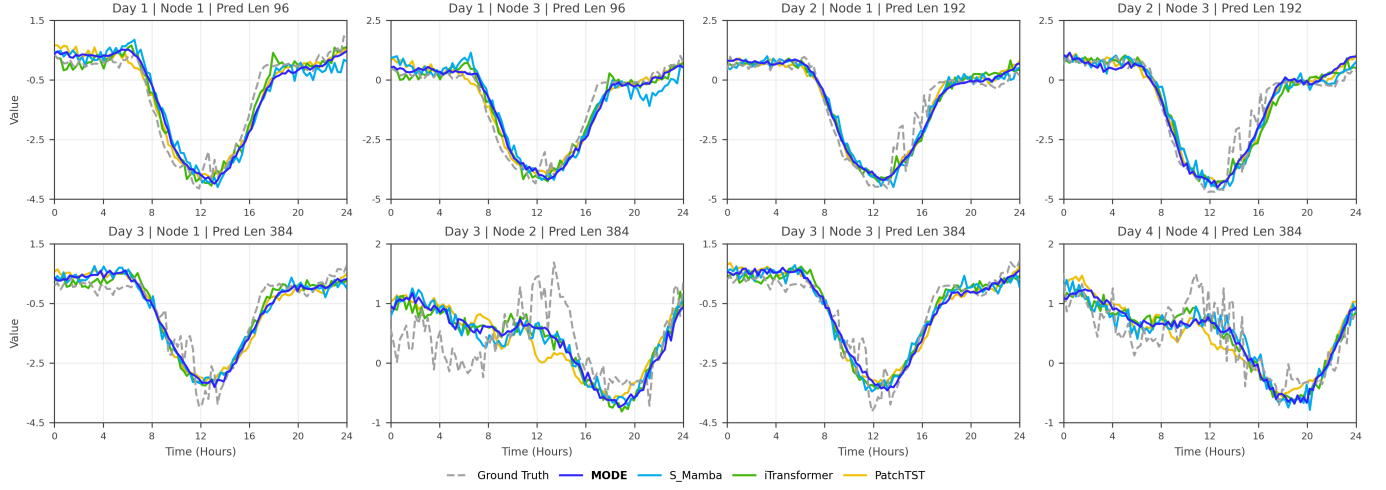


Fig. 6: Case study of **MODE** on ETTm1 across different horizons and scenarios.

dependencies, especially during transition periods where temperature changes rapidly. The method successfully reconstructs the smooth temperature curves while avoiding the erratic fluctuations observed in baseline approaches.

Consistency Across Different Scenarios: The case study encompasses various challenging conditions including different seasonal patterns (Day 1 vs Day 4) and varying prediction complexities. **MODE** consistently outperforms alternatives, demonstrating its robustness and generalization capability across diverse forecasting scenarios.

These qualitative results complement our quantitative analysis and provide compelling evidence of **MODE**’s effectiveness in capturing complex temporal dynamics for accurate time series forecasting.

IV. RELATED WORK

Modern time series forecasting has progressed rapidly with the development of deep sequence models, particularly Transformer-based architectures [15]. These models capture long-range temporal dependencies through the self-attention mechanism, enabling accurate multistep forecasting. Extensions of the Transformer framework [8, 14, 35] incorporate causal masking to preserve the temporal order, while hierarchical designs such as Pyraformer [9] and cross-variate modules like Crossformer [32] further enhance contextual representation. However, their quadratic time complexity $\mathcal{O}(N^2)$ and memory cost limit scalability to long sequences. To address this, numerous studies have explored linearized or window-based attention mechanisms, yet these often trade off precision for efficiency. Large-scale pretraining frameworks such as Moirai [19] offer another direction but differ substantially in setup and scale from our controlled evaluation.

Recently, Mamba-based architectures [5, 27, 29, 24, 26] have emerged as promising state-space models, demonstrating strong performance in temporal reasoning and long-context sequence modeling. While these methods improve computational efficiency, they remain limited in handling irregularly sampled sequences and continuous-time dynamics.

In contrast, our proposed **MODE** introduces the first unified framework that combines Low-Rank Neural Ordinary Differential Equations (Neural ODEs) with an Enhanced Mamba architecture. This integration enables continuous-time modeling, efficient long-range dependency capture, and adaptive computational allocation through selective scanning. By bridging the gap between ODE-based temporal modeling and scalable state-space architectures, **MODE** achieves state-of-the-art accuracy while maintaining superior efficiency and robustness compared to prior Transformer and Mamba variants.

V. CONCLUSION

In this work, we present **MODE**, a unified and efficient framework for time series forecasting that integrates Low-Rank Neural Ordinary Differential Equations (Neural ODEs) with the Mamba architecture. By combining the continuous-time modeling capabilities of Neural ODEs with Mamba’s selective scanning mechanism, **MODE** effectively captures long-range temporal dependencies, gracefully handles irregular sampling patterns, and substantially decreases computational overhead. The proposed low-rank parameterization further improves scalability by reducing the state-transition complexity from $\mathcal{O}(d^2)$ to $\mathcal{O}(d \cdot r)$, while preserving rich representational power. Extensive experiments on diverse benchmark datasets show that **MODE** consistently delivers state-of-the-art accuracy, efficiency, and robustness. Comprehensive ablation and robustness analyses validate each architectural component and confirm resilience to noise and long forecasting horizons. Future directions include integrating probabilistic inference and physics-informed priors for enhanced uncertainty quantification and broader real-world applicability.

REFERENCES

- [1] Marie Auger-Méthé, Ken Newman, Diana Cole, Fanny Empacher, Rowenna Gryba, Aaron A King, Vianey Leos-Barajas, Joanna Mills Flemming, Anders Nielsen, Giovanni Petris, et al. A guide to state-space modeling of ecological time series. *Ecological Monographs*, 91(4):e01470, 2021.

[2] Chenyi Chen, Jianming Hu, Qiang Meng, and Yi Zhang. Short-time traffic flow prediction with ARIMA-GARCH model. In *Intelligent Vehicles Symposium*, pages 607–612. IEEE, 2011.

[3] Abhimanyu Das, Weihao Kong, Andrew Leach, Shaan Mathur, Rajat Sen, and Rose Yu. Long-term forecasting with tide: Time-series dense encoder. *arXiv preprint arXiv:2304.08424*, 2023.

[4] Philippe Esling and Carlos Agon. Time-series data mining. *ACM Computing Surveys (CSUR)*, 45(1):1–34, 2012.

[5] Albert Gu and Tri Dao. Mamba: Linear-time sequence modeling with selective state spaces. *arXiv preprint arXiv:2312.00752*, 2023.

[6] Xinyu Huang, Jun Tang, and Yongming Shen. Long time series of ocean wave prediction based on patchtst model. *Ocean Engineering*, 301:117572, 2024.

[7] Zhe Li, Shiyi Qi, Yiduo Li, and Zenglin Xu. Revisiting long-term time series forecasting: An investigation on linear mapping. *arXiv preprint arXiv:2305.10721*, 2023.

[8] Bryan Lim and Stefan Zohren. Time-series forecasting with deep learning: a survey. *Philosophical Transactions of the Royal Society A*, 379(2194):20200209, 2021.

[9] Shizhan Liu, Hang Yu, Cong Liao, Jianguo Li, Weiyao Lin, Alex X Liu, and Schahram Dustdar. Pyraformer: Low-complexity pyramidal attention for long-range time series modeling and forecasting. In *International conference on learning representations*, 2021.

[10] Yong Liu, Tengge Hu, Haoran Zhang, Haixu Wu, Shiyu Wang, Lintao Ma, and Mingsheng Long. itransformer: Inverted transformers are effective for time series forecasting. *arXiv preprint arXiv:2310.06625*, 2023.

[11] Ganapathy Mahalakshmi, S Sridevi, and Shyamsundar Rajaram. A survey on forecasting of time series data. In *2016 international conference on computing technologies and intelligent data engineering (ICCTIDE’16)*, pages 1–8. IEEE, 2016.

[12] Larry R Medsker, Lakhmi Jain, et al. Recurrent neural networks. *Design and applications*, 5(64-67):2, 2001.

[13] Eric Nguyen, Karan Goel, Albert Gu, Gordon Downs, Preey Shah, Tri Dao, Stephen Baccus, and Christopher Ré. S4nd: Modeling images and videos as multidimensional signals with state spaces. *Advances in neural information processing systems*, 35:2846–2861, 2022.

[14] José F Torres, Dalil Hadjout, Abderrazak Sebaa, Francisco Martínez-Álvarez, and Alicia Troncoso. Deep learning for time series forecasting: a survey. *Big Data*, 9(1):3–21, 2021.

[15] Ashish Vaswani, Noam Shazeer, Niki Parmar, Jakob Uszkoreit, Llion Jones, Aidan N Gomez, Łukasz Kaiser, and Illia Polosukhin. Attention is all you need. *Advances in neural information processing systems*, 30, 2017.

[16] Zihan Wang, Fanheng Kong, Shi Feng, Ming Wang, Xiaocui Yang, Han Zhao, Daling Wang, and Yifei Zhang. Is mamba effective for time series forecasting? *Neurocomputing*, 619:129178, 2025.

[17] Zihan Wang, Fanheng Kong, Shi Feng, Ming Wang, Han Zhao, Daling Wang, and Yifei Zhang. Is mamba effective for time series forecasting? *arXiv preprint arXiv:2403.11144*, 2024.

[18] Qingsong Wen, Tian Zhou, Chaoli Zhang, Weiqi Chen, Ziqing Ma, Junchi Yan, and Liang Sun. Transformers in time series: A survey. *arXiv preprint arXiv:2202.07125*, 2022.

[19] Gerald Woo, Chenghao Liu, Akshat Kumar, Caiming Xiong, Silvio Savarese, and Doyen Sahoo. Unified training of universal time series forecasting transformers. *arXiv preprint arXiv:2402.02592*, 2024.

[20] Haixu Wu, Tengge Hu, Yong Liu, Hang Zhou, Jianmin Wang, and Mingsheng Long. Timesnet: Temporal 2d-variation modeling for general time series analysis. In *The eleventh international conference on learning representations*, 2022.

[21] Haixu Wu, Jiehui Xu, Jianmin Wang, and Mingsheng Long. Autoformer: Decomposition transformers with auto-correlation for long-term series forecasting. *Advances in neural information processing systems*, 34:22419–22430, 2021.

[22] Ailing Zeng, Muxi Chen, Lei Zhang, and Qiang Xu. Are transformers effective for time series forecasting? In *Proceedings of the AAAI conference on artificial intelligence*, volume 37, pages 11121–11128, 2023.

[23] Qianru Zhang, Xinyi Gao, Haixin Wang, Siu Ming Yiu, and Hongzhi Yin. Efficient traffic prediction through spatio-temporal distillation. In *Proceedings of the AAAI Conference on Artificial Intelligence*, volume 39, pages 1093–1101, 2025.

[24] Qianru Zhang, Liang Qu, Honggang Wen, Dong Huang, Siu-Ming Yiu, Nguyen Quoc Viet Hung, and Hongzhi Yin. M2rec: Multi-scale mamba for efficient sequential recommendation. *arXiv preprint arXiv:2505.04445*, 2025.

[25] Qianru Zhang, Haixin Wang, Cheng Long, Liangcai Su, Xingwei He, Jianlong Chang, Tailin Wu, Hongzhi Yin, Siu-Ming Yiu, Qi Tian, et al. A survey of generative techniques for spatial-temporal data mining. *arXiv preprint arXiv:2405.09592*, 2024.

[26] Qianru Zhang, Honggang Wen, Ming Li, Dong Huang, Siu-Ming Yiu, Christian S Jensen, and Pietro Liò. Autoformer: Efficient hierarchical autoregressive transformer for time series prediction. *arXiv preprint arXiv:2506.16001*, 2025.

[27] Qianru Zhang, Honggang Wen, Wei Yuan, Crystal Chen, Menglin Yang, Siu Ming Yiu, and Hongzhi Yin. Hmamba: Hyperbolic mamba for sequential recommendation. *arXiv preprint arXiv:2505.09205*, 2025.

[28] Qianru Zhang, Peng Yang, Junliang Yu, Haixin Wang, Xingwei He, Siu-Ming Yiu, and Hongzhi Yin. A survey on point-of-interest recommendation: Models, architectures, and security. *IEEE Transactions on Knowledge and Data Engineering*, 2025.

[29] Qianru Zhang, Chenglei Yu, Haixin Wang, Yudong Yan, Yuansheng Cao, Siu Ming Yiu, Tailin Wu, and Hongzhi Yin. Fldmamba: Integrating fourier and laplace transform decomposition with mamba for enhanced time series prediction. *arXiv preprint arXiv:2507.12803*, 2025.

- [30] Regina Zhang, Siqi Goh, Xingsheng Chen, Zongru Li, Honggang Wen, Jiale Guo, Menglin Yang, Hongzhi Yin, Qiang Yang, Siu Ming Yiu, and Kwok Yan Lam. From prompts to agents: A comprehensive survey of llm-driven time series analysis. 11 2025.
- [31] Regina Zhang, Yuting Sun, Honggang Wen, Peng Yang, Xinzhu Li, Ming Li, Kwok Yan Lam, Pietro Liò, Siu Ming Yiu, and Hongzhi Yin. Time series analysis in frequency domain: A survey of open challenges, opportunities and benchmarks. 2025.
- [32] Yunhao Zhang and Junchi Yan. Crossformer: Transformer utilizing cross-dimension dependency for multivariate time series forecasting. In *The eleventh international conference on learning representations*, 2022.
- [33] Yongsen Zheng, Jinghui Qin, Pengxu Wei, Ziliang Chen, and Liang Lin. Cipl: counterfactual interactive policy learning to eliminate popularity bias for online recommendation. *IEEE Transactions on Neural Networks and Learning Systems*, 2023.
- [34] Yongsen Zheng, Guohua Wang, Jinghui Qin, Ziliang Chen, Junfan Lin, Pengxu Wei, Liang Lin, and Kwok-Yan Lam. Cirec: Causal intervention-inspired policy learning to mitigate exposure bias for interactive recommendation. *IEEE Transactions on Knowledge and Data Engineering*, 2025.
- [35] Yongsen Zheng, Pengxu Wei, Ziliang Chen, Yang Cao, and Liang Lin. Graph-convolved factorization machines for personalized recommendation. *IEEE Transactions on Knowledge and Data Engineering*, 35(2):1567–1580, 2021.
- [36] Yongsen Zheng, Ruilin Xu, Ziliang Chen, Guohua Wang, Mingjie Qian, Jinghui Qin, and Liang Lin. Hycorec: Hypergraph-enhanced multi-preference learning for alleviating matthew effect in conversational recommendation. In *Proceedings of the 62nd Annual Meeting of the Association for Computational Linguistics (Volume 1: Long Papers)*, pages 2526–2537, 2024.
- [37] Yongsen Zheng, Ruilin Xu, Guohua Wang, Liang Lin, and Kwok-Yan Lam. Mitigating matthew effect: Multi-hypergraph boosted multi-interest self-supervised learning for conversational recommendation. In *Proceedings of the 2024 Conference on Empirical Methods in Natural Language Processing*, pages 1455–1466, 2024.
- [38] Haoyi Zhou, Jianxin Li, Shanghang Zhang, Shuai Zhang, Mengyi Yan, and Hui Xiong. Expanding the prediction capacity in long sequence time-series forecasting. *Artificial Intelligence*, 318:103886, 2023.
- [39] Haoyi Zhou, Shanghang Zhang, Jieqi Peng, Shuai Zhang, Jianxin Li, Hui Xiong, and Wancai Zhang. Informer: Beyond efficient transformer for long sequence time-series forecasting. In *The Thirty-Fifth AAAI Conference on Artificial Intelligence, AAAI 2021, Virtual Conference*, volume 35, pages 11106–11115. AAAI Press, 2021.
- [40] Tian Zhou, Ziqing Ma, Qingsong Wen, Xue Wang, Liang Sun, and Rong Jin. Fedformer: Frequency enhanced decomposed transformer for long-term series forecasting. In *International conference on machine learning*, pages 27268–27286. PMLR, 2022.